Available online at www.sciencedirect.com
ScienceDirect
International Journal of Heat and Mass Transfer 50 (2007) 2282–2295
International Journal of HEAT and MASS TRANSFER
www.elsevier.com/locate/ijhmt

Experimental study of compressibility, roughness and rarefaction influences on microchannel flow

G.H. Tang, Zhuo Li, Y.L. He, W.Q. Tao *

State Key Laboratory of Multiphase Flow, School of Energy and Power Engineering, Xi'an Jiaotong University, Xi'an, Shaanxi 710049, PR China

Received 4 January 2006; received in revised form 17 August 2006
Available online 28 December 2006

Abstract

The existing experimental data in the literature on friction factor in microchannels are analyzed. Flow characteristics for nitrogen and helium in stainless steel microtubes, fused silica microtubes and fused silica square microchannels are studied experimentally. The data in fused silica microtubes with diameters ranging from 50 to 201 μm and the data in fused silica square channels with hydraulic diameter ranging from 52 to 100 μm show that the friction factors are in good agreement with the theoretical predictions for conventional-size channels. The friction factors in stainless steel tubes ($D = 119$–300 μm) are much higher than the theoretical predictions for tubes of conventional size. This discrepancy is resulted from the large relative surface roughness in the stainless steel tubes. From the literature review and the present test data it is suggested that for gaseous flow in microchannels with a relative surface roughness less than 1% the conventional laminar prediction should still be applied. A positive deviation of the friction factor from the conventional theory is observed due to the compressibility effect. In addition, smaller friction factors in fused silica microtubes with inner diameters ranging from 10 to 20 μm are obtained and the decrease in friction factor from the rarefaction effect is observed.

Keywords: Microchannel; Friction factor; Roughness; Compressibility; Rarefaction

1. Introduction

In recent years, the application of micro-electro-mechanical-systems (MEMS) has been ever increasing in many fields due to the rapid development of fabrication technology. Devices having dimensions of the order of microns are being developed for such applications spreading from micro-electronic cooling systems, bipolar plates of fuel cell and compact heat exchangers to reactors for a range of processes and advanced propulsion systems. Generally, the classical thermal and fluid dynamic theories developed for macro-systems are not fully applicable to fluids in microscale structures. Velocity slip, thermal creep, viscosity dissipation, compressibility and other non-continuum effects should be considered synthetically for the flow in microchannels. Novel theories and correlations are needed for better understanding the characteristics of microscale transport phenomenon and for designing microdevices more efficiently [1].

A large number of experimental studies have been conducted for the flow and heat transfer in micorchannel, yet diversities and deviations still exist even for the very basic problem such as the friction constant of laminar flow in microchannels. This study tries to tentatively clarify the reasons which can account for such diversities in the measurement of friction characters.

The contents of the paper are organized as follows. In this section, a comprehensive review on the experimental measurement of friction data in laminar flow is reviewed, and the diversities between different test data are analyzed. Based on this review and analysis, the reasons which can account for such diversities and deviations are proposed. In order to further verify the proposed reasons, special

* Corresponding author. Tel./fax: +86 29 82669106.
E-mail address: wqtao@mail.xjtu.edu.cn (W.Q. Tao).

0017-9310/$ - see front matter © 2006 Elsevier Ltd. All rights reserved.
doi:10.1016/j.ijheatmasstransfer.2006.10.034

experimental measurements are conducted (Section 2) and the results are presented and analyzed (Section 3). Finally, some conclusions are drawn.

Wu and little [2] are ones of the pioneer investigators. They studied the gas flow characteristics in rectangular glass channels ($D_h = 45.5$–83.1 μm) and silicon channels ($D_h = 55.8$–72.4 μm). The gas friction factors obtained were substantially higher (about 10–30% higher in silica channels and 3–5 times in glass channels) than those predicted by the Moody chart and the transitional Reynolds number was found as low as 350. It is commonly believed that the significant deviations were attributed to the large relative roughness (ε/D_h) of the channels, about 20–30% as estimated on the basis of Karman correlation of the Moody diagram.

Lin et al. [3] studied R12 flow in two copper tubes with diameters of 0.66 and 1.17 mm and about 20% higher friction factor was obtained than that calculated by using the Blasius equation in the Reynolds number range of $4640 < Re < 37600$.

Urbanek et al. [4] studied liquid flow (propanol and pentanol) in silicon microchannels with hydraulic diameters of 12 and 25 μm. The experimental results indicated that the friction factor was temperature dependent and increased by 5–30% in the temperature range of 0–85 °C compared to the classical theoretical prediction.

Peng et al. [5] experimentally investigated the flow characteristics of water flow through rectangular stainless steel microchannels with hydraulic diameters ranging from 133 to 367 μm and width to height ratios from 0.333 to 1. Their results indicated that the flow transition occurred at Reynolds number 200–700. This transition Reynolds number decreased as the size of the microchannel decreased. The flow friction behaviors of both laminar and turbulent flows were found to deviate from the classical theories. The friction factors were either larger or smaller than the predictions and the geometries were found to have important effects on flow.

Experiments were conducted by Mala and Li [6] for stainless steel and fused silica microtubes with diameters of 50–254 μm and relative roughness of 0.69–3.5%. The tested Reynolds number ranged from 100 to 2000. In a whole, the experimental results were larger than those predicted by the conventional theory. The deviation increased with the decreasing diameter and the increasing Reynolds number. An early transition from laminar to turbulent flow at $300 < Re < 900$ was observed for microtubes with diameters of 50–150 μm.

Papautsky et al. [7] investigated water flow in rectangular metallic pipette arrays. Each array was consisted of 5 or 7 pipettes with widths varying from 150 to 600 μm and heights ranging from 22.7 to 26.3 μm. An approximate 20% increase over the classical theory prediction was observed in the friction constant at low aspect ratios.

Qu et al. [8] investigated water flow through trapezoidal silicon microchannels with hydraulic diameters of 51.3–168.9 μm when $Re < 1500$. The relative inner surface roughness was between 1.76% and 2.85%. The friction factor was 8–38% higher than the classical theory prediction for laminar flow.

Jiang et al. [9] tested a micro-heat exchanger composed of rectangular copper microchannels with a hydraulic diameter of 300 μm, and the surface roughness of the microchannels was between 5.8 and 36.3 μm and the corresponding relative roughness was 1.9–12.1%. The experimental friction factor was much higher than the convectional predictions both in laminar and turbulent flow. The flow transition also occurred much earlier ($Re = 600$).

Celata et al. [10] studied R114 flow in a stainless steel capillary tube with $D = 130$ μm and $\varepsilon/D = 2.65\%$ at a wide range of Reynolds numbers ($Re = 100$–8000). Friction factors were in good agreement with the Hagen–Poiseuille theory as long as the Reynolds number was below 585. For higher Reynolds numbers, friction factor deviated from the conventional theory to the higher side. The transition from laminar to turbulent agreed well with rough commercial tubes in the Reynolds number range of 1880–2480.

Brutin and Tadrist [11] studied water flow in silicon microtubes with $D = 50$–530 μm and relative roughness less than 0.02%. The tested friction factor increased for decreasing microtube diameter and was 27% higher than the conventional theoretical predictions for $D = 50$ μm tube.

Acosta et al. [12] studied nitrogen flow in a narrow rectangular stainless steel channel with $D_h = 953$ μm. There were five types of surfaces with relative roughness from 0.13% to 5.2%. In laminar regime, the friction factor in two channels with smaller roughness ($\varepsilon/D_h = 0.21\%$ and 0.31%) coincided with that in the smooth channel ($\varepsilon/D_h = 0.13\%$). The friction factor in the other two rough channels ($\varepsilon/D_h = 2.4\%$ and 5.2%) was considerably larger than that in the smooth channel.

Pfahler et al. [13] tested a larger silicon rectangular microchannel with width of 53 μm and depth of 135 μm and other smaller two silicon rectangular microchannels with both widths of 100 μm and depths of 1.7 and 0.8 μm. The friction factor in 135 μm deep channel and 1.7 μm deep channel for *n*-propanol flow was found to be in rough agreement with the theoretical predictions. However, the friction factor for 0.8 μm deep channel was three times greater than the theoretical prediction and it decreased with the increase in Reynolds number.

Pfund et al. [14] conducted experiments for water flow through rectangular microchannels with hydraulic diameters of 128–521 μm. Reynolds numbers were between 60 and 3450. For the channel with $D_h = 521$ μm and $\varepsilon/D_h = 0.57\%$, the friction factors were in rough agreement with the theoretical value and the increase is less than 8%. For three other channels with relative roughness between 1.14% and 5.71%, the increase in friction constant ranged from 10% to 25%.

Li et al. [15] studied water flow in glass microtubes ($79.9 < D < 166.3$ μm), silicon microtubes ($100.3 < D <$

205.3 μm), and stainless steel microtubes ($128.8 < D < 179.8$ μm) with Reynolds number below 4000. For glass and silicon microtubes, friction factors and transition Reynolds numbers were in good agreement with the classical theoretical predictions. For rough stainless steel microtubes, friction factors were 15–37% higher than the theoretical predictions in tubes with relatively smaller diameters while a rough agreement or a slight increase was observed for larger tubes. The measured relative roughness was less than 0.1% for glass and silicon microtubes and 3.3–3.9% for stainless steel microtubes.

Cui et al. [16] studied liquid flow in silicon microtubes with diameters ranging from 3 to 10 μm. The relative surface roughness was less than 0.7%. The Reynolds number ranged from 0.1 to 24. The friction factor for water was in good agreement with the conventional theory while the friction factors for isopropanol and carbon tetrachloride increased significantly with the increase of the pressure. The authors attributed it to the viscosity effect at high pressure.

Phares and Smedley [17] studied water, saline, and glycerol/water mixture in circular tubes. The relative surface roughness for four stainless steel tubes with $D = 164$–440 μm ranged from 2.5% to 1.8% and the relative surface roughness for two polyimide tubes with $D = 119$ and 152 μm was less than 1%. The measured friction factor in polyimide tubes was in good agreement with the theoretical prediction while the friction factor in stainless steel tubes had 17% deviation to the higher side.

Kandlikar et al. [18] experimentally studied hydraulic diameters of 325–1819 μm with Reynolds numbers ranging from 200 to 7200 for air and 200–5700 for deionized, degassed water. For smooth microchannel with relative roughness 0.13%, the experimental friction factor and transition Reynolds numbers were in good agreement with conventional theory. For relative roughness values of 6–14% based on the constricted flow diameter, the transition Reynolds number varied between the values of 800 and 350 for air and water, respectively, and occured at lower Reynolds number with an increase in the relative roughness. The tested friction factors were much higher than the conventional theory.

Nakagawa et al. [19] investigated DI water flow in 5 μm deep and 200–800 μm wide silicon rectangular channels. The experimental friction factor agreed within 10% with the conventional theoretical prediction.

Heun [20] studied nitrogen gas flow in silicon circular, square and triangular microchannels with hydraulic diameters ranging from 0.619 to 1.494 mm. The experimental results were in good agreement with the conventional theory in both laminar and turbulent flow regimes.

Jiang et al. [21] presented an experimental investigation of water flow through silicon microchannels including circular, rectangular and triangular cross-section shapes. The hydraulic diameter of microchannels ranged from 8 to 42 μm and Reynolds number from 0.1 to 2. They found that the friction factors agreed well with the classical theoretical predictions and no geometry influence on flow was observed.

Du et al. [22] studied nitrogen in glass microtubes ($79.9 < D < 166.3$ μm). The measured relative roughness was less than 0.1%. The friction factor and transition Reynolds number were in good agreement with classical theory predictions.

Xu et al. [23] studied water flow through rectangular aluminum channels with $46.8 < D_h < 344.3$ μm and silicon channels with $29.59 < D_h < 79.08$ μm for $20 < Re < 4000$. The relative roughness ranged from 0.15% to 1% for aluminum channels and ranged from 0.025% to 0.07% for silicon channels. Rough agreement with theoretical prediction in friction factor was reported.

Gao et al. [24] studied water flow in three rectangular microchannels with height of 0.1–1 mm over a Reynolds number range of 20–7400. The aspect ratio of the channel ranged from 25 to 250 and the measured relative roughness was less than 0.1%. The results showed that no scale effects were found. The friction factor was in good agreement with that in the conventional-size channels and the onset to turbulence occurred at a critical Reynolds number in the range of 2500–4000.

Judy et al. [25] investigated the distilled water, methanol, and isopropanol flow in silicon and stainless steel microchannels with round and square cross-section shape. The channel diameters were in the range of 15–150 μm. Distinguished deviation from classical theory was not observed among the experimental results over a Reynolds number range of 8–2300.

Li and Cui [26] investigated the non-ion water and several organic liquids (CCL_4, $C_6H_5C_2H_5$ and isopropyl alcohol, etc.) in silicon microtubes with diameters about 20 μm. The results showed that the flow rate behaviors for polar or non-polar liquids were in agreement with the conventional theory of Hagen–Poiseuille flow.

Wu and Cheng [27] measured friction factors of laminar flow for deionized water. The hydraulic diameters for the silicon microchannels with trapezoidal cross-section were in the range of 25.9–291 μm. The relative roughness of all tested microchannels was measured to be no more than 0.12%. The experimental data were found to be in good agreement with the classical predictions. For the channels with larger hydraulic diameters of 103.4–291 μm, transition from laminar to turbulent flow was found at $Re = 1500$–2000.

Yang et al. [28] provided a systematic test of friction behavior for air, water, and R134a in 10 tubes with diameters from 0.173 to 4.01 mm over a Reynolds number range of 200–30000. The test friction factors for water and R134a agreed well with the conventional Blasius and Poiseuille equations in turbulent and laminar regime. For air flow in smaller tubes at high Reynolds numbers, the Blasius equation developed for incompressible flow was no longer appropriate for friction prediction.

Lelea et al. [29] studied the distilled water behaviors through 0.1, 0.3, and 0.5 mm diameter stainless steel micro-

tubes when $Re < 800$. The authors concluded that the classical theories are applicable for water flow through microchannels of above sizes.

Sharp and Adrian [30] performed experiments for circular glass microtubes with diameters ranging from 50 to 247 μm. The working fluids were water, 1-propanol, and a 20% solution by weight of glycerol. The critical Reynolds number for transition and the pressure drop were consistent with the macroscale data.

Baviere et al. [31] studied water flow in silicon rectangular channels with height of 21–4.5 μm. The relative roughness ranged from 1.1% to 0.24% and the Reynolds number 0.1–300. The experimental friction factor was in good agreement with the theoretical prediction for conventional channels.

Kohl et al. [32] studied compressible flow (air) for $6.8 < Re < 18814$ and incompressible flow (water) for $4.9 < Re < 2068$ in the silicon channels with hydraulic diameters ranging from 25 to 100 μm. The relative roughness for the tested channels was between 0.29% and 1.3%. The experimental results suggest that friction factors for microchannels can be accurately determined from data for standard large channels.

Hegab et al. [33] studied refrigerant R134a flow in aluminum rectangular channels with hydraulic diameters of 112–210 μm and relative roughness ranging from 0.16% to 0.89%. Reynolds number ranged from 1280 to 13,000. For the few data points collected in the laminar regime, the experimental results for friction factor were very close to predictions using classical laminar flow theory, but in the transition and turbulent regimes, the friction factors were typically 9–23% lower than convectional correlations.

Harley et al. [34] conducted flow experiments for nitrogen, helium and argon flow through trapezoidal silicon microchannels with relative roughness height less than 0.97% ($D_h = 1.01$–35.91 μm). The average friction constant was within 3% of the theoretical prediction for $D_h = 19.18$ μm ($Re = 5$–1200) and 2%–18% lower for $D_h = 1.01$ μm as Reynolds number decreased from 0.43 to 0.012.

Pfahler et al. [35,36] performed experimental studies of liquid and gas flow in silicon rectangular and trapezoidal channels with hydraulic diameters of 0.96–39.7 μm and relative roughness less than 0.97%. For both liquids and gases, the friction factor was less than the theoretical value for conventional size channels and also lower for helium than nitrogen.

Choi et al. [37] measured nitrogen gas flow friction factors in silica microtubes with diameters of 3–81 μm at a Reynolds number range of 20–20000. The relative roughness in the microtubes ranged from 0.02% to 1.16%. The correlations of $fRe = 53$ for laminar and $f = 0.140Re^{-0.182}$ for turbulent were obtained from the experiments, which are 20% lower than macroscale value of 64 in laminar regime and 20% lower in turbulent regime, respectively.

In Ref. [38] by Arkilic et al., helium flow through a silicon microchannel with 1.33 μm deep, 52.25 μm wide and 7500 μm long was investigated. The measured relative roughness was less than 0.05%. The mass flow rate was increased compared with no-slip model prediction, which implied that the friction resistance was reduced.

Nitrogen and water flow in silicon microtubes with diameters of 19, 25 and 102 μm was reported by Yu et al. [39]. The measured relative roughness in the microtubes was less than 0.03%. Nitrogen and water friction factor was about 19% lower than the theoretical value of 64 for $Re < 2000$. The friction constant correlation of $fRe = 50.13$ was obtained. For turbulent regime ($Re = 6000$–20000), the reduction of about 5% in the friction constant was observed.

Shih et al. [40] measured the local pressure distribution of nitrogen and helium flow in a silicon microchannel with height 1.2 μm and width 40 μm. The mass flow rate was increased and the friction factor was reduced compared with classical theoretical prediction.

Turner et al. [41] investigated helium and nitrogen flow in silica rectangular channels with hydraulic diameters of 9.7, 19.6, and 46.6 μm and relative roughness of 0.011–0.2% at a Reynolds number range of 0.2–1000. The gas local pressure distribution in the microchannel was measured. The friction constant (fRe) was roughly equal to 60%, 40% lower than the classical theoretical prediction. They believed that the low friction factor was due to eliminating entrance pressure losses in the experiment.

Li et al. [42] measured flow rate and pressure distribution for nitrogen flow in two constriction microdevices, an orifice and a Venturi with hydraulic diameter 1.1 μm fabricated on silicon substrates. The microchannel outlet Knudsen number was about 0.06. The measured mass flow rate was in good agreement with the first-order slip model and was increased compared to the conventional theory.

In Ref. [43], Araki et al. also investigated friction characteristics of nitrogen, argon and helium flow through silicon microtubes with $D = 5$–100 μm. In the tested Reynolds number range of 0.03–29.7, the measured friction constant floated from 63 to 50. The largest deviation was 20% lower than the theoretical prediction value of 64.

Arkilic et al. [44] also studied nitrogen, argon and CO_2 flow through a silicon microchannel with 1.33 μm deep. The measured relative roughness was less than 0.05%. The measured mass flow rate was increased compared with no-slip model prediction which indicated that the friction resistance was reduced.

Araki et al. [45] studied helium and nitrogen flow in triangle and trapezoidal silicon microchannels with $D_h = 3.92$–10.3 μm and $\varepsilon/D < 0.364\%$. The flow resistance in trapezoidal channels was observed to be lower than that in conventional size channels. The reduced flow resistance was ascribed to the rarefaction effect due to extremely small dimensions. For triangle microchannels, the flow resistance was higher than the conventional size channels and the possible explanation was the presence of three-dimensional flow structures.

Hsieh et al. [46] studied nitrogen gas flow in a silicon channel with 50 μm deep and 200 μm wide. The inlet Knudsen number ranged from 0.001 to 0.02 and the Reynolds number ranged from 2.6 to 89.4. The measured relative roughness was less than 0.5%. The results were found in good agreement with those predicted by analytical solutions in which a 2-D continuum flow model with first-order slip boundary conditions were employed.

Colin et al. [47] studied nitrogen and helium flow in silicon rectangular microchannel with the depths ranging from 4.5 to 0.5 μm and aspect ratio from 1% to 9%. The tested outlet Knudsen number was less than 0.25. A good agreement with the second-order slip model has been found for all the data.

We summarized the above-mentioned experimental results in the literature into three categories: the one for which the friction constant is larger than the conventional theoretical predictions, the one in rough agreement with the conventional theoretical predictions, and the one lower than the conventional theoretical predictions in Tables 1–3, respectively (in the table, a and b mean partial results in the reference). From Table 1 it can be observed that most of the reported surface relative roughness is larger than 1%. The exceptions are the data in [11] and [16], where the friction factors are higher than conventional theoretical predictions even if the relative roughness is less than 0.02% for water [11] and less than 0.7% for polar fluids at high pressure [16]. The surface roughness data are not reported in Refs. [3–5,7,13] and hence no further comments can be made.

In Table 2, the experimental results are in rough agreement with the conventional theoretical predictions. It can be found that the relative surface roughness reported usually being less than 1%. The roughness data were not reported in Refs. [13,19–21,25,28–30], hence no judgment can be conducted.

In Table 3, the experimental results are smaller than the classical theoretical predictions. It is found that the reported relative roughness is usually less than 1% except for [40,42,43,47] where the roughness data were not provided.

Table 1
Summary of the experimental results larger than conventional theoretical predictions in the literature

References	Relative roughness (%)
Wu and Little [2]	20–30
Lin et al. [3]	NA
Urbanek et al. [4]	NA
Peng et al. [5]	NA
Mala and Li [6]	0.69–3.5
Papautsky et al. [7]	NA
Qu et al. [8]	1.76–2.85
Jiang et al. [9]	1.9–12.1
Celata et al. [10]	2.65
Brutin and Tadrist [11]	<0.02
Acosta et al. [12]b	2.4; 5.2
Pfahler et al. [13]b	NA
Pfund et al. [14]b	1.14; 2.33; 5.71
Li et al. [15]b	3.3–3.9
Cui et al. [16]b	<0.7; isopropanol, carbon tetrachloride
Phares and Smedley [17]b	2.5–1.8
Kandlikar et al. [18]b	6–14

Table 2
Summary of the experimental results in rough agreement with conventional theoretical predictions in the literature

References	Relative roughness (%)
Acosta et al. [12]a	0.13; 0.31; 0.21
Pfahler et al. [13]a	NA
Pfund et al. [14]a	0.57
Li et al. [15]a	<0.1
Cui et al. [16]a	<0.7; DI water
Phares and Smedley [17]a	<1
Kandlikar et al. [18]a	0.13
Nakagawa et al. [19]	NA
Heun [20]	NA
Jiang et al. [21]	NA
Du et al. [22]	< 0.1
Xu et al. [23]	Aluminum: 0.15–1; silicon: 0.025–0.07
Gao et al. [24]	<0.1
Judy et al. [25]	NA
Cui and Li [26]	<0.7
Wu and Cheng [27]	<0.12
Yang et al. [28]	NA
Lelea et al. [29]	NA
Sharp and Adrian [30]	NA
Baviere et al. [31]	1.1–0.24
Kohl et al. [32]	0.29–1.3
Hegab et al. [33]	0.16–0.89
Harley et al. [34]a	<0.97

In addition, by carefully inspecting the test data it is found that apart from the relative surface roughness effect, the outlet Knudsen number for the gaseous flows also influences the flow character. The test data in Table 3 are higher than 0.001 and the flow is in the slip or marginal transitional regime. While in Ref. [22], nitrogen flow in microtubes is still in continuum regime because its outlet Knudsen number is within 0.0004–0.0008, and the friction factors were reported to be in good agreement with theoretical predictions.

Therefore, we may tentatively conclude that the higher relative roughness (say, $\varepsilon/D_h > 1\%$) is responsible for the higher friction behaviors in microchannels while the relatively higher Knudsen number (flow in slip or transition regime) is responsible for the lower friction behaviors for gas flows in microchannels. Generally speaking, roughness of metallic microchannels is larger than that of silicon or glass microchannels. And this may account for the fact that the measured friction constant in silicon or glass microchannels is usually smaller than that in metallic microchannels.

To verify the above argument on the effects of the relative surface roughness and rarefaction, in this paper two series of measurements are conducted. First, nitrogen and helium flows in fused silica microtubes ($D = 50$–201 μm), square microchannels ($D_h = 52$–100 μm) and stainless steel microtubes ($D = 119$–300 μm) are measured to verify the roughness effect. Second, nitrogen and helium flow in fused

Table 3
Summary of the experimental results lower than conventional theoretical predictions in the literature

References	Relative roughness (%)	Knudsen number	Working fluid
Harley et al. [34]b	<0.97	0.001–0.4	N_2; Ar; He
Pfahler et al. [35,36]	<0.97	0.014–0.363	Isopropyl alcohol; silicone oil; N_2; He
Choi [37]	0.02–1.16	NA	N_2
Arkilic et al. [38]	<0.05	0.165	He
Yu [39]	<0.03	NA	N_2; water
Shih et al. [40]	NA	N_2: 0.055; He: 0.16	N_2; He
Turner [41]	0.011–0.2	N_2: 0.0028–0.014; He: 0.0084–0.04	N_2; He
Li et al. [42]	NA	0.06	N_2
Araki et al. [43]	NA	N_2: 0.00648–0.031; He: 0.0136–0.0345	N_2; Ar; He
Arkilic et al. [44]	<0.05	0.03–0.44	N_2; Ar; CO_2
Araki et al. [45]	<0.364	>0.001	N_2; He
Hsieh et al. [46]	<0.5	Inlet Knudsen number: 0.001–0.02	N_2
Colin et al. [47]	NA	<0.25	N_2; He

silica microtubes with smaller diameters of 10–20 μm is studied to verify the rarefaction effect. Then based on these measurements, the comprehensive effects of roughness, compressibility and rarefaction on microchannel flow behaviors are discussed. Finally, some conclusions are stated.

2. Experimental setup

The experimental test system is depicted schematically in Fig. 1. The detailed descriptions for components and measurement apparatus are listed in Table 4. To avoid clogging, pressurized gas from the gas tank (1) flows through a 0.5 μm filter (4) before entering the test section (6). Two sumps (5) at the inlet and the outlet of the test section are fabricated to connect the test microtube. The inlet pressure is controlled by a coarse pressure regulator (2) and a precision regulator (3). The absolute pressure and temperature in the two sumps are measured by two absolute pressure transducers (A1, A2) and two T-type copper-constantan thermocouples (B), respectively. After discharging from the test section, the gas passes through a volume flow meter (C1–C4) with different flow rate ranges selected by a switching ball valve (8). Finally, the exit gas vents to the atmosphere directly.

Because of the very small size of the channel, the thermal equalization time between the gas temperature and that of the wall is very short and heat interaction occurs rapidly between the gas and the environment, so that the temperature of the gas is treated as though it were essential constant and equal to the temperature of the environment, i.e., isothermal flow is assumed. In fact, due to viscous dissipation effect, the gas temperature rise from channel inlet to outlet was observed and the difference increased with gas velocity, but never exceeded 3 °C in the test. The measured inlet and outlet values were averaged to determine a representative temperature for the fluid.

For the one-dimensional, isothermal and compressible flow, the average friction factor f_c for the duct length L between Ma_1 and Ma_2, is given as follows [48]

$$f_c = \frac{D_h}{L}\left[\frac{Ma_2^2 - Ma_1^2}{\gamma Ma_1^2 Ma_2^2} - \ln\left(\frac{Ma_2}{Ma_1}\right)^2\right] \quad (1)$$

where γ is the specific heat ratio. Further discussion on this equation will be provided in the later presentation. In the experiment, we neglect the entrance developing region effect on the average friction factor by using microchannels with relative large ratios of length to hydraulic diameter. This approximation holds on especially for small-size

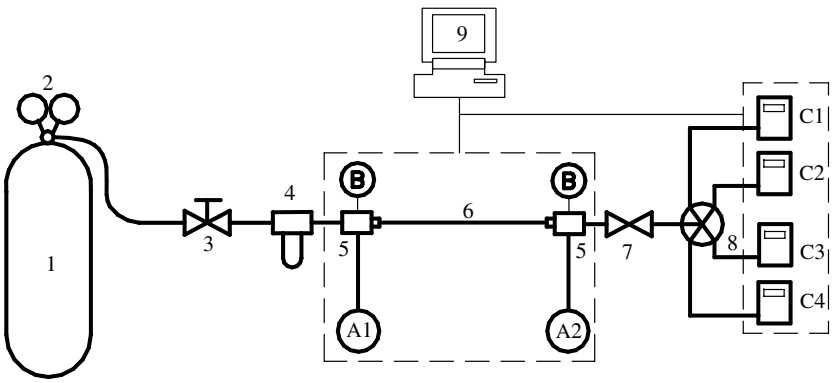

Fig. 1. Schematic of the experimental loop.

Table 4
Flow loop components

Label	Description	Manufacturer/model	Range	Accuracy
1	Gas tank	Messer	15 MPa	
2	Pressure regulator	Shanghai regulator Factory/YQD-6		
3	Precision regulator	Swagelok/SS-SS4		
4	Filter	Swagelok/SS-4F-05		0.5 μm
5	Connection Adapter for test section	In-house construction		
6	Test section			
7	Plug valves	Swagelok/SS-4P4T		
8	5-way switching ball valve	Swagelok/SS-43ZFS2		
9	Computerized data acquisition system	Solartron/35951C		
A1	Absolute pressure transducer	ZFBY3801	0–1 MPa	0.25%
A2	Absolute pressure transducer	ZFBY3801	0–0.25 MPa	0.25%
B	Thermocouples	T-type copper-constantan/omega	0–200 °C	0.5 °C
C1	Volumetric flow meter	Cole-Parmer/3290702	0–5 ml/min	2%
C2	Volumetric flow meter	Cole-Parmer/3290706	0–50 ml/min	2%
C3	Volumetric flow meter	Cole-Parmer/3290712	0–500 ml/min	2%
C4	Volumetric flow meter	Cole-Parmer/3290715	0–5000 ml/min	2%

channels. For large-size channels at high Reynolds number, the neglect will bring on some errors. With regard to the minor losses, approximate analysis using incompressible flow theory for macroscale channels shows that the inlet minor loss is $0.25\rho u^2$ [49]. Because the inlet velocity is not large, especially for small-size channels, the inlet minor loss accounts for a quite small part in the total pressure drop and thus can be neglected. However, the outlet pressure loss cannot be neglected and is estimated using the above mentioned equation.

Eleven different circular and square microchannels listed in Table 5 are tested in the experiment. The typical cross-section and longitudinal-section photos by a scanning electron microscope (SEM) are shown in Fig. 2. By using light-section microscope, we measured the surface relative roughness of the test fused silica channels which is significantly smaller than 1%. And the absolute average surface roughness of the four stainless steel tubes is 7 μm.

To assess the accuracy of measurement, we performed an uncertainty analysis since each measurement device has some uncertainty associated with it. Calculated values such as Reynolds number and friction factor have an uncertainty based on the individual uncertainties of each measured value used in the calculation. The uncertainty of the Reynolds number and the friction factor, generally denoted by δy, is determined by the root-sum-square expression [50].

$$y = f(x_1, x_2, \ldots, x_N)$$
$$\delta y = \left[\left(\frac{\partial f}{\partial x_1}\delta x_1\right)^2 + \ldots + \left(\frac{\partial f}{\partial x_N}\delta x_N\right)^2\right]^{1/2} \quad (2)$$

where δ_{x_1} to δ_{x_N} are the measurement uncertainties for each device. The uncertainties of measurement devices for flow parameter are listed in Table 4 and those for the channel dimension are listed in Table 5.

By applying Eq. (2), the calculated mean uncertainty for the Reynolds number and friction factor are 4.5% and 5.9%, respectively.

Table 5
Dimensions of fused silica tubes (FST), stainless steel tubes (SST), fused silica square channels (FSC), and fused silica microtubes (MFST) tested in the experiment

Tube/channel	Hydraulic diameter $D \pm 1$ μm	Length $L \pm 0.02$ mm	*Re*	Outlet *Ma*	Outlet *Kn*
FST1	201.44	100.40	28–6200	0.017–0.6	1.6×10^{-4}–9.8×10^{-4}
FST2	102.74	93.02	33–3100	0.04–0.6	2.8×10^{-4}–1.9×10^{-3}
FST3	74.36	49.42	7–2700	0.012–0.6	3.5×10^{-4}–2.6×10^{-3}
FST4	50.55	50.28	6–1200	0.015–0.6	8.1×10^{-4}–3.9×10^{-3}
FSC1	100.25	74.14	60–3600	0.05–0.6	2.6×10^{-4}–1.4×10^{-3}
FSC2	75.34	49.66	7–2700	0.01–0.6	3.5×10^{-4}–2.6×10^{-3}
FSC3	52.03	33.62	24–2000	0.05–0.6	4.3×10^{-4}–3.7×10^{-3}
SST1	300.00	100.00	81–5200	0.22–0.6	2.1×10^{-4}–2.2×10^{-4}
SST2	260.00	100.00	81–5000	0.19–0.6	1.8×10^{-4}–2.6×10^{-4}
SST3	172.00	100.02	14–2700	0.015–0.58	2×10^{-4}–8.8×10^{-4}
SST4	119.09	99.76	14–4900	0.01–0.6	3.5×10^{-4}–1.6×10^{-3}
MFST1	19.78 ± 0.5	27.50	4–230	0.025–0.44	0.0028–0.01
MFST2	14.54 ± 0.3	29.92	9–230	0.075–0.52	0.0035–0.014
MFST3	10.06 ± 0.3	29.72	3–70	0.04–0.3	0.0065–0.02

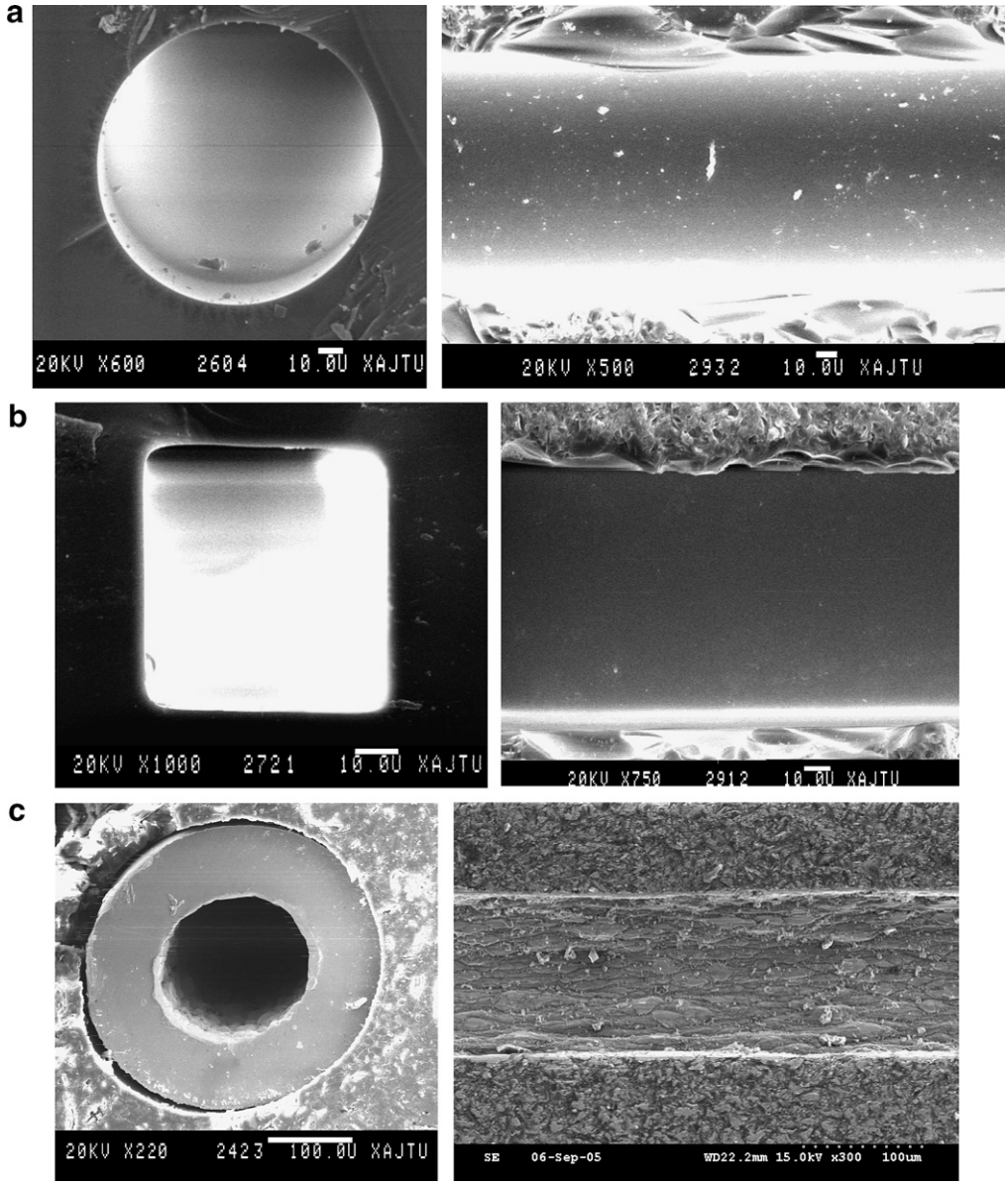

Fig. 2. SEM images of three typical tested tubes: (a) a fused silica microtube with $D = 102$ μm; (b) a fused silica square microchannel with $D_h = 52$ μm; (c) a stainless steel microtube with $D = 172$ μm.

3. Results and discussion

3.1. Friction factor and roughness effect

The friction factor calculated by Eq. (1) is plotted against Reynolds number in Figs. 3–5. Fig. 3 presents the friction factor for nitrogen and helium flow in fused silica microtubes with different inner diameters. The tested friction factor in microtubes is compared with that from Poiseuille flow prediction for incompressible, laminar flow in a conventional-sized tube, $f = 64/Re$. For the turbulent regime, prediction from Blasius equation, $f = 0.316/Re^{0.25}$, is used for comparison. Fig. 4 shows the experimental results for nitrogen and helium flow in fused silica square microchannels. Analytical results for f provided by Shah and London [51] for various aspect ratios, α, have been curve-fitted and following equation is obtained which is adopted to determine the incompressible friction factor for square channels of normal size according to its value of aspect ratio:

$$f_{inc} = \frac{96}{Re}(1 - 1.355\alpha + 1.946\alpha^2 - 1.7012\alpha^3 + 0.9564\alpha^4 - 0.2537\alpha^5) \quad (3)$$

For the turbulent regime, Filonenko equation [52] of the following form is used for comparison.

$$f = (1.82 \lg Re - 1.64)^{-2} \quad (4)$$

Fig. 5a–d shows the experimental results for nitrogen and helium flow in the stainless steel microtubes.

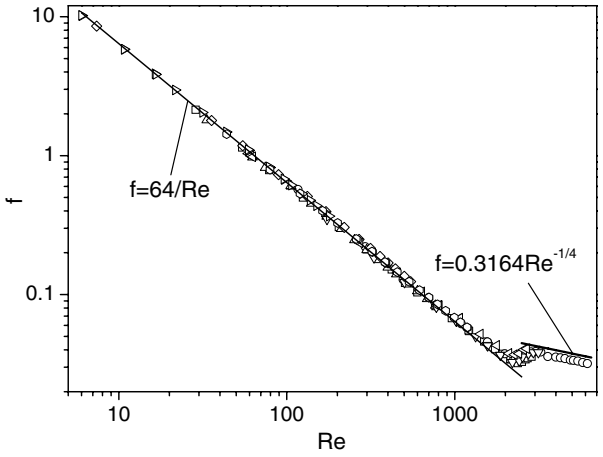

Fig. 3. Experimental friction factor for helium and nitrogen flow in FST1 ($D = 201$ μm), FST2 ($D = 102$ μm), FST3 ($D = 74$ μm), and FST4 ($D = 50$ μm).

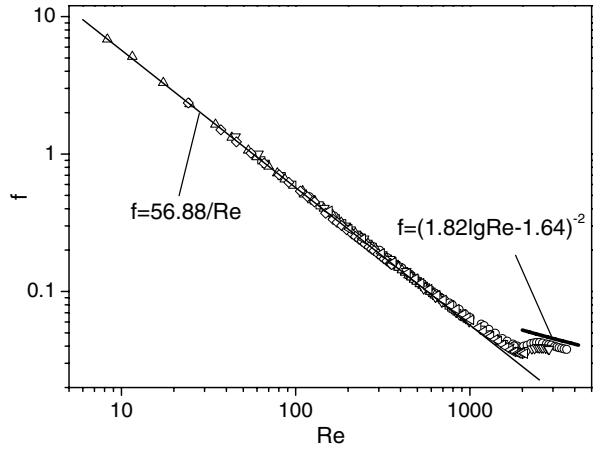

Fig. 4. Experimental friction factor for helium and nitrogen flow in FSC1 ($D_h = 100$ μm), FSC2 ($D_h = 75$ μm), and FSC3 ($D_h = 52$ μm).

As shown in Figs. 3 and 4, in the laminar flow regime all the experimental results show good agreement with the predictions except in the higher Reynolds number regime. The deviation occurring at the high Reynolds number regime looks like that the flow is transiting to a turbulent one. The transition is slightly earlier than that observed in the conventional-size systems. Within the tube/channel sizes studied there is no clear size-related increase or decrease trend for the deviation between the experimental results and the theoretical predictions. Analyzing the outlet Mach number of the channel, we find that the outlet Mach number reaches as high as 0.5–0.6 in the high Reynolds number regime. Thus it is expected that the compressibility effect should cause the deviation. According to Guo et al. [53], the compressibility effect increase the mean velocity in the streamwise direction and thus bring on an additional pressure drop due to gas acceleration. The gas compressibility would lead to an increasing friction factor with the increase of Mach number or Reynolds number. The compressibility makes the curve of f against Re for the present experimental data deviate from the curve of $fRe = \text{constant}$, especially at relative high Reynolds number. It looks like an earlier transition from laminar to turbulent flow.

In Fig. 5a–d, it is obvious that the friction factor for stainless steel tubes is significantly higher than the theoretical prediction for conventional sized tubes. In the laminar regime, the friction factor is about 28%, 33%, 55%, and 70% higher for the tubes of $D = 300$, 260, 172, and 119 μm, respectively. We attribute this result to surface roughness effect. Comparing the cross-sections and longitudinal sections of the SEM photos for the stainless steel tubes with the fused silica tube or square channel shown in Fig. 2, we find that the inner surface of the stainless steel tubes is very irregular and many concavo-convex particles are present, while the inner surface of the fused silica tubes can be regarded as hydraulically smooth. Comparing the experiment data with the Churchill equation [54],

$$\frac{1}{\sqrt{f}} = 19.656 \ln\left(\frac{1}{0.888\sqrt{f}/Re + 0.27\varepsilon/D}\right) \tag{5}$$

we can estimate the relative roughness which is 3.2%, 3.8%, 6.5%, and 9.5% for the tubes of $D = 300$, 260, 172, and 119 μm, respectively. From these estimated relative roughness, the absolute roughness height can be obtained which is in the range about 9.6–11.3 μm. However, as indicated above the measured absolute roughness of the present tubes is 7 μm with light-section microscope. The corresponding relative roughness is 2.3%, 2.7%, 4.1%, and 5.9% for the four tubes of $D = 300$, 260, 172, and 119 μm, respectively, which are about one third smaller than the predictions from the Churchill correlation. We attribute this difference to the roughness density distribution (including roughness shape, spacing, etc.) in the inner surface of the microchannels. It seems that Churchill's equation for conventional size commercial tubes is not applicable for predicting friction behaviors for rough microchannels. According to the traditional theory, the surface roughness has negligible effect on the friction factor for laminar flow [55,56]. The above conclusion was partially based on the observation of Nikuradse's sand roughness experiments. Bradshaw [57] argued that Nikuradse's sand roughness actually consisted of grains of nearly uniform size, quite unlike the wide distribution of element sizes found in most rough surfaces and in nature or in engineering. Ahn [58] studied the effect of different roughness shape geometries experimentally and he found that the effects of roughness shape and distributed-density on friction factor were significant. It is believed that the effect of roughness shape and distribution on microchannel flow is more important. It is worth noting that in Fig. 5, the experimental curve for laminar flow is not parallel to the curve of $f = 64/Re$, the difference between them gets larger as the Reynolds number increases. But the degree of the increase is somewhat different from that of roughness effect on conventional size channels, for the latter the difference increases very largely with the Reynolds number observed

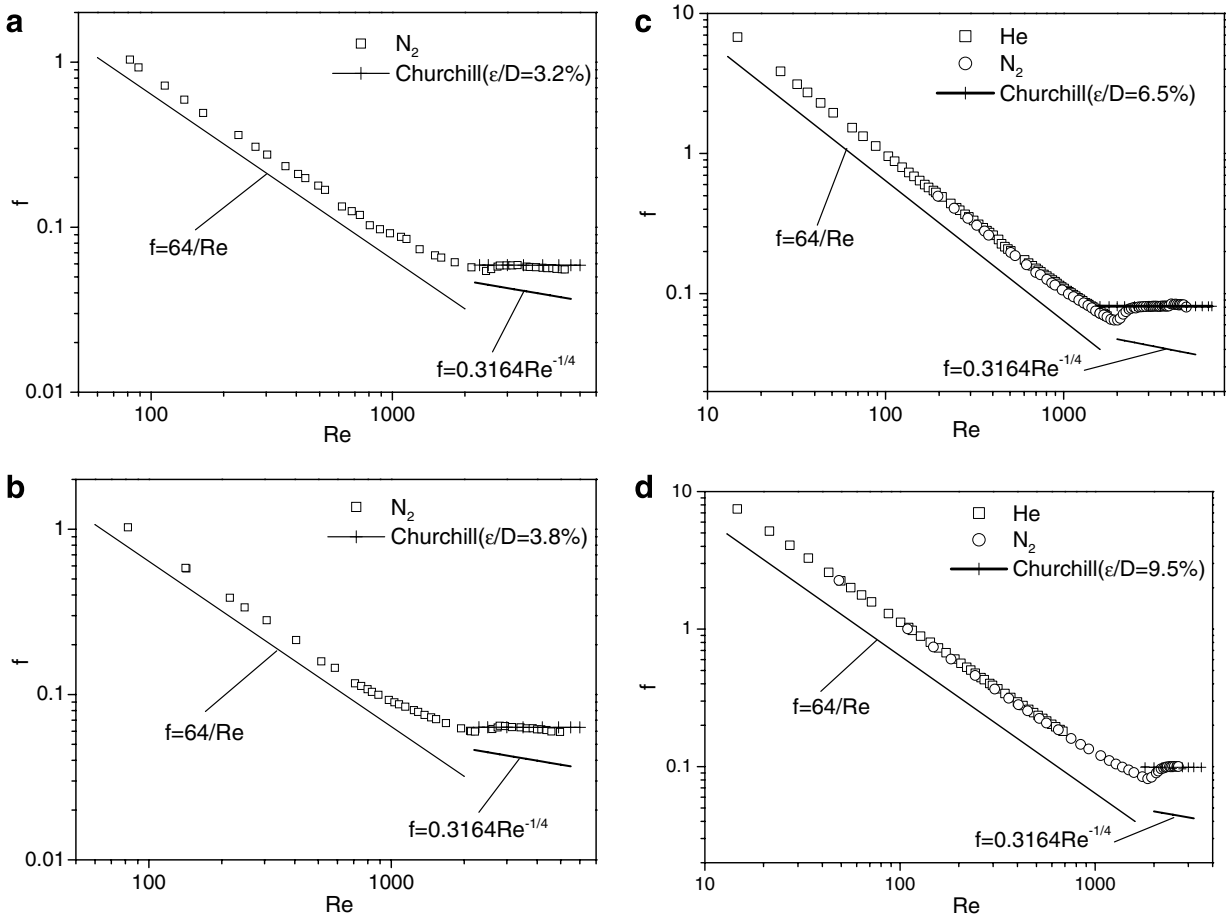

Fig. 5. Experimental friction factor for four microchannels: (a) SST1 ($D = 300$ μm); (b) SST2 ($D = 260$ μm); (c) SST3 ($D = 172$ μm); (d) SST4 ($D = 119$ μm).

in conventional flow. As described above, in the tested microchannels, the relative roughness height is not very large, but the roughness element distributes quite densely at the inner surface. The authors believe that this fact could partially explain the difference between the roughness effect of the present microchannels and that of conventional size ones. Of course, part of the possible explanation could be the measurement uncertainty on the channel size. The existence of roughness makes the accurate measurement of the inner diameter very difficult.

From above presentation, following conclusions may be made. For laminar flow in microchannels, the relative surface roughness has a significant effect on the friction constant. For the gaseous flow in smooth microchannels (relative surface roughness less than about 1%) with $D_h > 50$ μm and outlet Knudsen number within 1.4×10^{-4} to 4×10^{-3}, the theoretical prediction for macroscale ducts can also be applied.

3.2. Compressibility effect

In the transport of a gas by microchannels, great changes in properties of the gas occur because of large pressure drop caused by the friction effects even when the flow velocity is small. For example, pressure drops of several atmospheres were observed in a 4 mm long channel [40] due to the viscous friction. Friction contributes to large pressure gradient, which in turn generates changes in gas density. In order to satisfy mass conservation, the gas must accelerate as its density decreases with the decreasing pressure towards the exit of the channel. Acceleration effect on the total pressure drop caused by the change of density must be considered. Thus, the pressure difference in the microchannel is made up of two parts: viscous friction and acceleration loss associated with the increase in the specific volume. Thus when test data are used to determine the friction factor, the acceleration loss should be separated. Note that in Eq. (1) for determining the friction factor the first term on the right-hand side represents the friction pressure drop and the second term represents the flow acceleration effect.

Fig. 6 shows the compressibility effect on friction factor. The experimental friction constant, fRe, normalized by the theoretical prediction is plotted against mean Mach number of the channel inlet and outlet. All the experimental data in fused silica tubes (FST) and square channels (FSC) for Reynolds number less than 2200 are presented. As the Mach number increases, the normalized value has

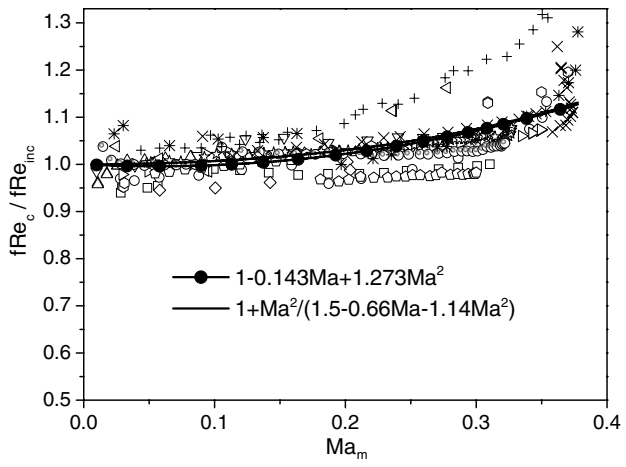

Fig. 6. Friction constant ratio of compressible flow to theoretical prediction for FST and FSC as a function of mean Mach number.

a slight increase in the small Mach number regime. The increase in the ratio steepens when the mean Mach number is higher than 0.25. Thus, it suggests that the compressibility effect should cause the deviation of flow characteristics from the conventional laminar prediction in the higher Reynolds number regime (about at $Re = 2000$) in Figs. 3 and 4. The test data in Fig. 6 has been curve-fitted following equation:

$$\frac{(fRe)_c}{(fRe)_{inc}} = (1 - 0.143Ma + 1.273Ma^2) \tag{6}$$

The solid circles in Fig. 6 indicate this increasing trend with the Mach number From this equation the friction constant increases by 15% at $Ma = 0.4$. In Fig. 6, a solid line is shown which depicts the analytical solutions in a microtube with perturbation method provided in [53],

$$\frac{(fRe)_c}{(fRe)_{inc}} = \left(1 + \frac{Ma^2}{1.5 - 0.66Ma - 1.44Ma^2}\right) \tag{7}$$

It can be seen that the agreement between the analytical solution and the experimental curve fit is very good.

3.3. Rarefaction effect

Rarefaction effect may be significant for gaseous flow in microchannels. The Knudsen number, Kn, defined as $Kn = \lambda/L$, provides a direct indication on whether the continuum approach can be applied or not as it compares the mean free path of molecules, λ, to the characteristic length, L. The continuum model is valid when the mean free path is much smaller than a characteristic flow dimension. A flow is considered as a continuum one when $Kn < 0.001$. As this condition is violated, the flow is no longer near equilibrium and the linear relation between stress and rate of strain and the no-slip boundary condition are no longer valid. Beyond that, the collision frequency is simply not high enough to ensure equilibrium and a certain degree of tangential-velocity slip in the streamwise direction must be considered [1]. For $Kn > 10$ the system can be considered as a free molecular flow and direct solution of the Boltzmann equation or gas dynamic model such as DSMC is required. The intermediate values of $0.1 < Kn < 10$ are associated with a transitional flow regime while those within the range of $0.001 < Kn < 0.1$ are representative of a slip flow regime. The Navier–Stokes and the energy equations may be applied to flows within the slip regime or marginally transitional regime in conjunction of the slip velocity and temperature jump boundary conditions at the wall.

As the Knudsen number increases, rarefaction effect becomes more significant and thus pressure drop, shear stress and corresponding mass flow rate cannot be predicted from the continuum models. To date, most studies have shown that the rarefaction effect generates the slip velocity at the wall and thus the shear stress reduces and the mass flow rate increases.

To verify the rarefaction effect, we tested three smaller fused silica microtubes (MFST1, MFST2 and MFST3). Fig. 7a and b show the friction constant ratio ($fRe/64$) of helium and nitrogen, respectively, as a function of

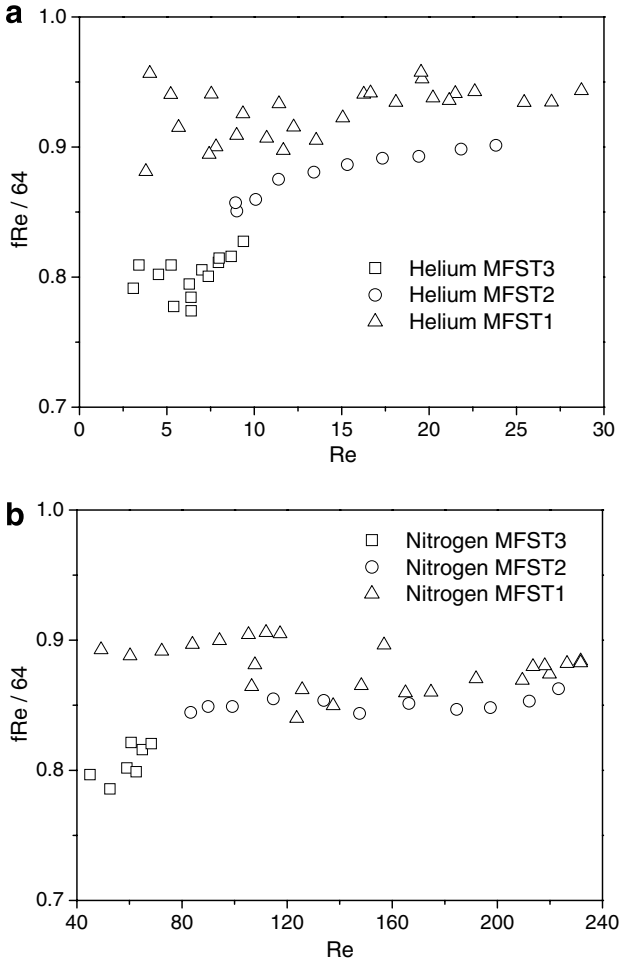

Fig. 7. The ratio of measured friction constant to theoretical value ($fRe/64$) as a function of Reynolds number. (a) Helium. (b) Nitrogen.

Reynolds number. It can be clearly seen that friction constants are reduced significantly in the three microtubes. Moreover, it can also be observed that the friction constant increases with the increase in Reynolds number with the trend in Fig. 7a being more obvious than that in Fig. 7b. This result can be explained as follows. In our experiments, the channel outlet pressure is fixed. Then the Reynolds number increase implies the increase in the inlet pressure, and the rarefaction level along the channel decreases, leading to the increase in the friction constant. Fig. 8 depicts friction constant for helium and nitrogen flow as a function of mean Knudsen number between inlet and outlet. The theoretical prediction of friction constant, given by the following Maxwell slip model [59] is also shown for comparison

$$f = \frac{64}{Re(1 + 8Kn(2 - \sigma_v)/\sigma_v)} \tag{8}$$

where σ_v is the tangential momentum accommodation coefficient, which represents the fractions of molecules experiencing diffuse reflection and thus the degree of slip at the wall. This coefficient depends on the fluid, the solid and the surface finish and has been determined experimentally to be between 0.2 and 0.8 [1].

It can be seen from Fig. 8 that generally the friction constant decreases as the Knudsen number increases. However, the absolute magnitude of the reduction in friction constant is larger than the prediction by the Maxwell slip model if σ_v is assumed to be unity. If $\sigma_v = 0.6$ for helium and $\sigma_v = 0.2$ for nitrogen are adopted, the experimental data can roughly fit the predictions of Maxwell slip model. The similar result has also been observed by Araki et al. [43]. Their measured friction factor for nitrogen flow in microtubes was obviously less than the prediction of Maxwell slip model at $\sigma_v = 1$. As indicated above, most experiments have verified that gas rarefaction effect reduces the flow resistance, but there are still disagreements for the absolute magnitude of the reduction. In addition, to determine the value of the tangential momentum accommodation coefficient, the common way is to compare experimental data with the first-order or second-order analytical solutions. However, for the same experimental results if compared with different analytical solutions the resulted tangential momentum accommodation coefficients are different. Therefore, further research work is needed to determine the quantitative rarefaction effect on microchannel flow.

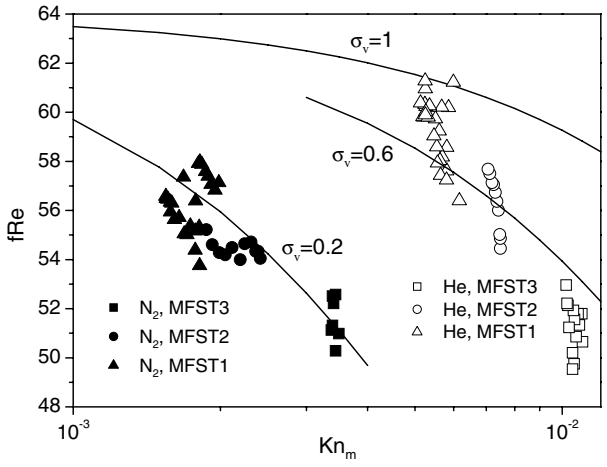

Fig. 8. Friction constant (fRe) as a function of mean Knudsen number between inlet and outlet for helium (He) and nitrogen (N_2) flow. The solid lines represent the predictions of Maxwell slip model at different momentum accommodation coefficients.

The Knudsen number can also be expressed in terms of Reynolds number and Mach number [1]

$$Kn = \frac{\lambda}{D_h} = \sqrt{\frac{\pi\gamma}{2}}\frac{Ma}{Re} \tag{9}$$

Thus, accounting for the roughness, rarefaction and compressibility effects, the gaseous flow friction factor in microchannels should be expressed like the following form,

$$f = F\left(Ma, Kn, \frac{\varepsilon}{D_h}, \varepsilon_{distrib}, \alpha\right) \tag{10}$$

where ε represents absolute roughness, $\varepsilon_{distrib}$ represents the roughness geometry parameters and α represents the effect of the channel geometry.

4. Conclusions

This paper presents experimental results to reveal the effects of surface roughness, compressibility and rarefaction on the friction factor of gaseous flow in microchannels. Frictional characteristics of nitrogen and helium flow in 11 different sized microchannels (FST, FSC, SST) with hydraulic diameters between 50 and 300 μm have been measured. The tested outlet Knudsen number ranges from 1.4×10^{-4} to 4×10^{-3}, and the tested outlet Mach number ranges from 0.01 to 0.6. The gaseous flow friction factor in stainless steel tube (SST) is observed to be much higher than the theoretical prediction for conventional size tubes while the friction factor in the fused silica tubes and fused silica channels (FST, FSC) agrees well with the theoretical prediction. The increase in friction factor is attributed to the dense roughness distribution in the inner surface of the stainless steel tubes. Surface roughness in microchannels is found to affect the friction factor. From the literature review and our test data it is suggested that for gaseous flow in microchannels with a relative surface roughness less than 1%, the conventional laminar prediction should still be applied.

Because of the gas compressibility effect, a positive deviation in the friction factor from the conventional incompressible flow theory are observed. By using curve fitting method, a correlation of $(fRe)_c/(fRe)_{inc}$ as a function of the Mach number for laminar flow is obtained.

For the smaller microtubes (MFST) with inner diameter ranging from 10 to 20 μm and the tested outlet Knudsen

number range of 0.003–0.02, the reduction in friction factor is observed in the experiment, which confirms that the rarefaction effect dominates the slip or transition flow and leads to the reduction of the friction factor. However, there are still disagreements for the absolute magnitude of the reduction. Further study is highly required in order to determine the rarefaction effect on the microflows in the slip or transition regime quantitatively.

The focus of this paper is concentrated on gas flow. For liquid microchannel experimental studies in Refs. [7,11] show that the polar fluid may have important effect on flow characteristics in very small microchannels. Numerical simulations for such cases are now underway and will be reported in the future.

Acknowledgements

This work was supported by the National Natural Science Foundation of China (Grant Nos. 50236010, 50406020, 50425620). The authors thank Prof. G.X. Wang of the University of Akron for helpful suggestions.

References

[1] M. Gad-el-Hak, The fluid mechanics of microdevices – the freeman scholar lecture, J. Fluids Eng. 121 (1999) 5–33.
[2] P.Y. Wu, W.A. Little, Measurement of the friction factors for the flow of gases in very fine channels used for microminiature Joule–Thomson refrigerators, Cryogenics 23 (1983) 273–277.
[3] S. Lin, C.C.K. Kwok, R.Y. Li, Z.H. Chen, Z.Y. Chen, Local frictional pressure drop during vaporization through capillary tubes, Int. J. Multiphase Flow 17 (1991) 95–102.
[4] W. Urbanekt, J.N. Zemel, H. Bau, An investigation of the temperature dependence of Poiseuille numbers in microchannel flow, J. Micromech. Microeng. 3 (1993) 206–208.
[5] X.F. Peng, G.P. Peterson, B.X. Wang, Frictional flow characteristics of water flowing through rectangular channels, Exp. Heat Transfer 7 (1994) 249–264.
[6] G.M. Mala, D.Q. Li, Flow characteristics of water in microchannels, Int. J. Heat Fluid Flow 20 (1999) 142–148.
[7] I. Papautsky, B.K. Gale, S. Mohanty, T.A. Ameel, A.B. Frazier, Effects of rectangular microchannel aspect ratio on laminar friction constant, in: Proceedings of the Society of Photo-optical Instrumentation Engineers (SPIE), vol. 3877, 1999, pp. 147–158.
[8] W.L. Qu, G.M. Mala, D.Q. Li, Pressure-driven water flows in trapezoidal silicon microchannels, Int. J. Heat Mass Transfer 43 (2000) 353–364.
[9] P.X. Jiang, M. H Fan, G.S. Si, Z.P. Ren, Thermal-hydraulic performance of small scale micro-channel and porous-media heat-exchangers, Int. J. Heat Mass Transfer 44 (2001) 1039–1051.
[10] G.P. Celata, M. Cumo, M. Guglielmi, G. Zummo, Experimental investigation of hydraulic and single – phase heat transfer in 0.130-mm capillary tube, Microscale Thermophys. Eng. 6 (2002) 85–97.
[11] D. Brutin, L. Tadrist, Experimental friction factor of a liquid flow in microtubes, Phys. Fluids 15 (2003) 653–661.
[12] R.E. Acosta, R.H. Muller, C.W. Tobias, Transport Processes in narrow (capillary) channels, AIChE J. 31 (1985) 473–482.
[13] J. Pfahler, J. Harley, H. Bau, Liquid transport in micron and submicron channels, Sensor Actuator A21–A23 (1990) 431–434.
[14] D. Pfund, D. Rector, A. Shekarriz, A. Popescu, J. Welty, Pressure drop measurement in a microchannel, AIChE J. 46 (2000) 1496–1507.
[15] Z.X. Li, D.X. Du, Z.Y. Guo, Experimental study on flow characteristics of liquids in circular microtubes, Microscale Thermophys. Eng. 7 (2003) 253–265.
[16] H.H. Cui, Z.H. Silber-Li, S.N. Zhu, Flow characteristics of liquids in microtubes driven by a high pressure, Phys. Fluids 16 (2004) 1803–1810.
[17] D.J. Phares, G.T. Smedley, A study of laminar flow of polar liquids through circular microtubes, Phys. Fluids 16 (2004) 1267–1272.
[18] S.G. Kandlikar, D. Schmitt, A.L. Carrano, J.B. Taylor, Characterization of surface roughness effects on pressure drop in single-phase flow in minichannels, Phys. Fluids 17 (2005) 100606-11.
[19] S. Nakagawa, S. Shoji, M. Esashi, A micro chemical analyzing system integrated on silicon chip, in: Proceedings IEEE Micro Electro Mechanical Systems, Napa Valley CA, 1990, pp. 89–94.
[20] M.K. Heun, Performance and optimization of microchannel condensers, Ph.D. Thesis, University of Illinois at Urbana-Champaign, 1995.
[21] X.N. Jiang, Z.Y. Zhou, J. Yao, Y. Li, X.Y. Ye, Micro-fluid flow in microchannels, in: The Eighth International Conference on Solid-State Sensors and Actuators and Erosensors, vol. IX, 1995, pp. 317–320.
[22] D.X. Du, Z.X. Li, Z.Y. Guo, Friction resistance for gas flow in smooth microtubes, Sci. China Ser. E-Technol. Sci. 43 (2000) 171–177.
[23] B. Xu, K.T. Ooi, N.T. Wong, Experimental investigation of flow friction for liquid flow in microchannels, Int. Comm. Heat Mass Transfer 27 (2000) 1165–1176.
[24] P.Z. Gao, S.L. Person, M. Favre-Marinet, Hydrodynamics and heat transfer in two-dimensional microchannels, Proceedings of 12th International Heat Transfer Conference, vol. 2, Grenoble, France, 2002, pp. 183–188.
[25] J. Judy, D. Maynes, B.W. Webb, Characterization of friction drop for liquid flows through microchannels, Int. J. Heat Mass Transfer 45 (2002) 3477–3489.
[26] Z.H. Li, H.H. Cui, Proceeding of experiments about liquid flow through microtubes, Int. J. Nonlinear Sci. Numer. Simult. 3 (2002) 577–580.
[27] H.Y. Wu, P. Cheng, Friction factor in smooth trapezoidal silicon microchannels with different aspect ratios, Int. J. Heat Mass Transfer 46 (2003) 2519–2525.
[28] C.Y. Yang, J.C. Wu, H.T. Chien, S.R. Lu, Friction characteristics of water, R134a, and air in small tubes, Microscale Thermophys. Eng. 7 (2003) 335–348.
[29] D. Lelea, S. Nishio, K. Takano, The experimental research on microtube heat transfer and fluid flow of distilled water, Int. J. Heat Mass Transfer 47 (2004) 2817–2830.
[30] K.V. Sharp, R.J. Adrian, Transition from laminar to turbulent flow in liquid filled microtubes, Exp. Fluids 36 (2004) 741–747.
[31] R. Baviere, F. Ayela, S. Le Person, M. Favre-Marinet, Experimental characterization of water flow through smooth rectangular microchannels, Phys. Fluids 17 (2005) 098105-4.
[32] M.J. Kohl, S.I. Abdel-Khalik, S.M. Jeter, D.L. Sadowski, An experimental investigation of microchannel flow with internal pressure measurements, Int. J. Heat Mass Transfer 48 (2005) 1518–1533.
[33] H. Hegab, A. Bari, T. Ameel, Friction and convection studies of R134a in microchannels within the transition and turbulent regimes, Exp. Heat Transfer 15 (2002) 245–259.
[34] J.C. Harley, Y.F. Huang, H.H. Bau, J.N. Zemel, Gas flow in microchannels, J. Fluid Mech. 284 (1995) 257–274.
[35] J. Pfahler, J. Harley, H.H. Bau, J.N. Zemel, Liquid and gas transport in small channel, MicroStruct. Sensor Actuator 19 (1990) 149–157.
[36] J. Pfahler, J. Harley, H.H. Bau, J.N. Zemel, Gas and Liquid flow in small channel, Micromech. Sensor Actuator 32 (1991) 49–60.
[37] S.B. Choi, R.F. Barron, R.O. Warrington, Fluid flow and heat transfer in microtubes, Micromech. Sensor Actuator 32 (1991) 123–134.

[38] E.B. Arkilic, K.S. Breuer, M.A. Schmidt, Gaseous flow in microchannels, Appl. Microfabricat. Fluid Mech. 197 (1994) 57–66.
[39] D. Yu, R. Warrington, R. Barron, T. Ameel, An experimental and theoretical investigation of fluid and heat transfer in microtubes, in: Proceedings of the 4th ASME/JSME Thermal Engineering Joint Conference, vol. 1, 1995, pp. 523–530.
[40] J.C. Shih, C.M. Ho, J.Q. Liu, Y.C. Tai, Monatomic and polyatomic gas flow through uniform microchannels, Microelectromechanical Syst. 59 (1996) 197–203.
[41] S.E. Turner, H.W. Sun, M. Faghri, Local pressure measurement of gaseous flow through microchannels, Proc. ASME Heat Transfer Div. vol. 364-3 (1999) 71–79.
[42] X.X. Li, Y.L. Lee, M. Wong, Y. Zohar, Gas flow in constriction microdevices, Sensor Actuator 83 (2000) 277–283.
[43] T. Araki, M.S. Kim, K. Inaoka, K. Suzuki, An experimental investigation of gaseous flow characteristics in micro-tubes, JSME Int. J. Ser. B-Fluids Thermal Eng. 43 (2000) 634–639.
[44] E.B. Arkilic, K. Breuer, M.A. Schmidt, Mass flow and tangential momentum accommodation in silicon micromachined channels, J. Fluid Mech. 437 (2001) 29–43.
[45] T. Araki, M.S. Kim, H. Iwai, K. Suzuki, An experimental investigation of gaseous flow characteristics in microchannels, Microscale Thermophys. Eng. 6 (2002) 117–130.
[46] S.S. Hsieh, H.H. Tsai, C.Y. Lin, C.F. Huang, C.M. Chien, Gas flow in a long microchannel, Int. J. Heat Mass Transfer 47 (2004) 3877–3887.
[47] S. Colin, P. Lalonde, R. Caen, Validation of a second-order slip flow model in rectangular microchannels, Heat Transfer Eng. 25 (2004) 23–30.
[48] M.A. Saad, Compressible Fluid Flow, Prentice-Hall, New Jersey, 1985.
[49] V.L. Streeter, E.B. Wylie, Fluid Mechanics, McGraw-Hill, New York, 1985.
[50] R.B. Abernethy, R.P. Benedict, R.B. Dowdell, ASME measurement uncertainty, ASME J. Fluids Eng. 107 (1985) 161–164.
[51] R.K. Shah, A.L. London, Laminar flow forced convection in ducts, in: Advances in Heat Transfer – Supplement 1, Academic Press, New York, 1978.
[52] V. Gnielinski, New equations for heat and mass transfer in turbulent pipe and channel flows, Int. Chem. Eng. 16 (1976) 359–368.
[53] Z.Y. Guo, Z.X. Li, Size effect on microscale single-phase flow and heat transfer, Int. J. Heat Mass Transfer 46 (2003) 149–159.
[54] S.W. Churchill, Friction-factor equation spans all fluid-flow regimes, Chem. Eng. 84 (1977) 91–92.
[55] H. Schlichting, Boundary Layer Theory, McGraw-Hill, New York, 1979.
[56] F.M. White, Fluid Mechanics, fifth ed., McGraw-Hill, New York, 2003, pp. 363–364.
[57] P. Bradshaw, A note on "critical roughness height" and "transitional roughness", Phys. Fluids 12 (2000) 1611–1614.
[58] S.W. Ahn, The effects of roughness types on friction factors and heat transfer in roughened rectangular duct, Int. Comm. Heat Mass Transfer 28 (2001) 933–942.
[59] W.A. Ebert, E.M. Sparrow, Slip flow in rectangular and annular ducts, ASME J. Basic Eng. 87 (1965) 1018–1024.